

This is the accepted manuscript made available via CHORUS. The article has been published as:

Surface melting of electronic order in
 $\text{La}_{0.5}\text{Sr}_{1.5}\text{MnO}_4$

S. B. Wilkins, X. Liu, Y. Wakabayashi, J.-W. Kim, P. J. Ryan, H. Zheng, J. F. Mitchell, and J. P. Hill

Phys. Rev. B **84**, 165103 — Published 7 October 2011

DOI: [10.1103/PhysRevB.84.165103](https://doi.org/10.1103/PhysRevB.84.165103)

Surface Melting of Electronic Order in $\text{La}_{0.5}\text{Sr}_{1.5}\text{MnO}_4$

S. B. Wilkins,¹ X. Liu,¹ Y. Wakabayashi,² J.-W. Kim,³ P. J. Ryan,³ J. F. Mitchell,⁴ and J.P. Hill¹

¹*Department of Condensed Matter Physics and Materials Science,
Brookhaven National Lab, Upton, New York 11973-5000, USA*

²*Osaka University, Division of Materials Physics,
Graduate School of Engineering Sciences, Osaka 5608531, Japan*

³*Argonne National Laboratory, Advanced Photon Source, 9700 S Cass Ave, Argonne, IL 60439 USA*

⁴*Argonne National Laboratory, Division of Materials Science, 9700 S Cass Ave, Argonne, IL 60439 USA*

(Dated: September 12, 2011)

We report temperature-dependent surface x-ray scattering studies of the orbital ordered surface in $\text{La}_{0.5}\text{Sr}_{1.5}\text{MnO}_4$. We find that as the bulk ordering temperature is approached from below, the thickness of the interface between the electronically ordered and electronically disordered regions at the surface grows, though the bulk correlation length remains unchanged. Close to the transition, the surface is so rough that there is no well-defined electronic surface, despite the presence of bulk electronic order. That is, the electronic ordering at the surface has melted. Above the bulk transition, long range ordering in the bulk is destroyed but finite-sized isotropic fluctuations persist, with a correlation length roughly equal to that of the low temperature in-plane surface correlation length..

PACS numbers:

I. INTRODUCTION

Bulk crystals can disorder on warming through one of two scenarios: surface melting or surface freezing. In the first, the surface of the solid melts at a lower temperature than the bulk. This is a common and even useful property of condensed matter and is, for example, what allows a skier to glide across the snow¹. In the second, the bulk melts at a lower temperature than the surface, a phenomenon seen in certain normal alkanes^{2,3}. An as yet unanswered question is, what happens when the order is not that of a crystal lattice, but rather is that of electronic order? This is a particularly important question on the nanoscale where the surface properties are dominant. For crystalline order, it has long been understood that nanoparticles should⁴ and do⁵ exhibit surface melting, though there remains much to be understood⁶. However, there has been little work to date on electronic order. We show here that, for a model system, namely orbitally ordered, single crystal, $\text{La}_{0.5}\text{Sr}_{1.5}\text{MnO}_4$ (LSMO), that the electronic order exhibits surface melting.

The temperature dependence of electronic order at a surface or interface is of fundamental interest since it can provide important insights into the nature of electronic interactions, and in particular the relative strength of the surface and bulk interactions. Nor is this question entirely academic. Next-generation devices that rely on electronic order will require understanding and control of electron transport across such surfaces at finite temperature. Thus this is a question of some importance.

Here, we use orbital order at the surface of a strongly correlated transition metal oxide as an exemplar system for studying electronic order at a surface. Before proceeding, it is important to define what we mean by a surface. The crystallographic surface is the surface between the solid crystal and the vacuum, as obtained by

cleaving the crystal. The electronic surface is the surface between the orbitally-ordered bulk and an orbitally disordered region located below the crystallographic surface. We refer to this as the ‘orbital surface’. There has been much work associated with the ground state behavior of such surfaces, starting with the original suggestion that “electronic reconstruction” can occur at the electronic order-disorder interface⁷. Surface effects in electronic order have been seen in such cases as the ferromagnetic surface of bilayer manganites⁸, the interface between ferromagnetic and superconducting oxides⁹, the orbital surface of manganites¹⁰ and the interface between LAO/STO heterostructures¹¹. However, it is not only the form of the electronic surface that is important, but also its evolution with temperature. Many strongly correlated systems exhibit significant functionality, such as CMR, in the vicinity of a phase transition. Therefore, understanding the electronic surface behavior upon crossing a phase transition is vitally important. To date there has been little work on the evolution of the electronic surface on warming through the bulk ordering temperature. The purpose of this work is to redress this imbalance.

We report temperature-dependent surface x-ray scattering studies of the orbitally ordered surface in LSMO. We find that the thickness of the interface between the electronically ordered and disordered regions at the surface grows as the bulk ordering temperature is approached from below, while the bulk correlation length remains unchanged, suggesting that the surface starts to roughen while the bulk is well ordered. Close to, but below, the transition, the surface is so rough that there is no well-defined electronic surface despite the presence of bulk electronic order: the electronic ordering at the surface has melted. Above the bulk transition, finite-sized isotropic fluctuations of orbital order are observed, with a correlation length equal to that of the surface in-plane

correlation length at the transition temperature. These results have important implications for the behavior of electronic surface at finite temperatures and we discuss these in view of potential future devices.

LSMO has been studied extensively in the bulk, revealing long range orbital order below ~ 240 K, with 3D magnetic order appearing below ~ 120 K^{12,13}. This orbital ordering gives rise to concomitant lattice distortions and thus may be studied utilizing x-ray scattering techniques. Specifically, by measuring the distribution of the scattering around the orbital-order superlattice reflection, one obtains information about the bulk order parameter. Information about the orbital surface comes from the “orbital truncation rods”¹⁰. These are rods of scattering normal to the surface connecting orbital superlattice peaks and are analogous to crystal truncation rods^{14,15} which result from the termination of a 3D crystal by a surface. The intensity distribution of the orbital-truncation-rods provides quantitative information on the interfacial roughness (interfacial width) and the in-plane correlations at the orbital surface.

II. EXPERIMENTAL

The experiments were carried out on beamline 6ID-B at the Advanced Photon Source. The incident photon energy was 12 keV. A single crystal of LSMO, grown in a floating zone furnace, was post-cleaved in air to reveal a [001] surface and immediately placed into the vacuum of a closed-cycle refrigerator. Q_z was along the surface normal. Scans were performed using a 4+2 diffractometer¹⁶, allowing access to the (2.25, -0.25, L) orbital rod and the (2.25, -0.25, 2) orbital Bragg peak. An incidence angle of 0.6° was used for all measurements and was chosen to be just slightly higher than the critical angle for total external reflection. The sample was indexed with $a = b = 3.78$ Å and $c = 12.4$ Å. Momentum transfer is either denoted as Q_x, Q_z in units of Å⁻¹, or L, in units of r.l.u., where 1 r.l.u. = 0.507 Å⁻¹. Measurements of the (2.25, -0.25, L) orbital-truncation rod were made by scanning along Q_x , perpendicular to the Q_z direction. A 2-D mesh of the intensity obtained from a series of such scans, collected at 170 K, is shown in the top right panel of Fig. 1. The top left hand side of Fig. 1 shows a simulation of the expected intensity of the superlattice reflection, in the absence of the orbital truncation rod, constructed from a 2D Lorentzian-squared function with Q_z and Q_x widths equal to the values measured at the (2.25, -0.25, 2) bulk superlattice reflection. The bottom panels show line cuts through the respective meshes. It is immediately apparent that the two behaviors are quite different; the observed scattering does not originate from tails of the orbital Bragg peak, but rather is the orbital truncation rod¹⁰.

Figure 2 shows two Q_x scans through this orbital truncation rod, taken at $Q_z = 0.1$ Å⁻¹ and 0.28 Å⁻¹, for two temperatures, $T = 170.0$ K and 223.5 K, i.e. well below,

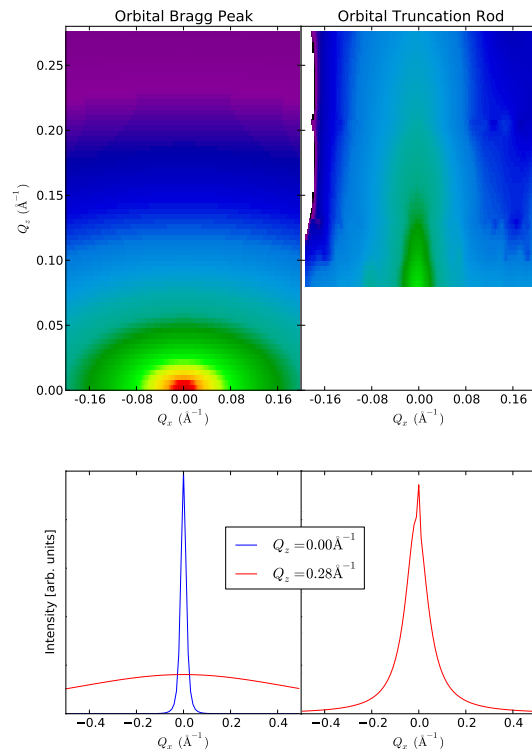


FIG. 1: (color online) (Top left) Simulated x-ray scattering in the (Q_x, Q_z) plane for a 2D Lorentzian-squared function, with widths equal to those of the bulk orbital order reflection. (Bottom left) Line cuts at $Q_z = 0$ Å⁻¹ (blue) and $Q_z = 0.28$ Å⁻¹ (red) through the simulated x-ray scattering intensity. (Top right) 2D Intensity plot of the measured intensity for the orbital truncation rod in $\text{La}_{0.5}\text{Sr}_{1.5}\text{MnO}_4$ at 170 K obtained at $Q_z = 0.101, 0.127, 0.202$ and 0.278 Å⁻¹. The streak of scattering, elongated along L due to the truncation of the orbital order by its surface can clearly be seen. (Bottom right) Line cut at $Q_z = 0.28$ Å⁻¹ through the orbital truncation rod.

and just below, the bulk ordering temperature, $T_{OO} = 226$ K. At low temperatures, a two-component lineshape is observed in the truncation rod scattering. This immediately implies that the orbital surface has a well-defined average height but finite in-plane correlations at the surface^{10,14}. We refer to these two components as the sharp and broad components. In the theory of a nearly-smooth surface¹⁴, the sharp component results from the average surface, and the intensity variation of this component as a function of Q_z is a measure of the roughness, or interfacial width, of that surface. A rough surface results in a faster decay of the sharp component intensity with Q_z , compared to that of a perfectly smooth surface. The broad component on the other hand, results from the finite in-plane correlation length of the surface, with a width inversely proportional to that correlation length. The rate of increase of the integrated intensity of the broad component as a function of Q_z increases with increasing interfacial roughness. We find that the two

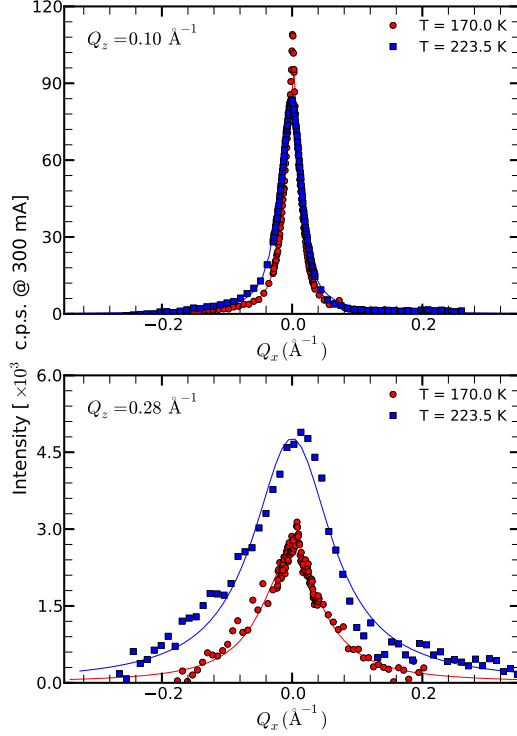


FIG. 2: (color online) (Top panel) Q_x scans through the orbital truncation rod at 170 K and 223.5 K (red circles and blue squares respectively). Data taken at $Q_z = 0.1 \text{ \AA}^{-1}$ (Top panel) and $Q_z = 0.28 \text{ \AA}^{-1}$ (Bottom panel). The results of the fits to Eq. 1 are shown as solid lines.

length-scale scattering is best fit by a Lorentzian-squared function for the sharp component and a Lorentzian function for the broad component:

$$I_T = I_S \left[\frac{\Gamma_S^2}{Q_x^2 + \Gamma_S^2} \right]^2 + I_B \left[\frac{\Gamma_B^2}{Q_x^2 + \Gamma_B^2} \right] \quad (1)$$

where I_S and I_B are the peak intensities of the sharp and broad components respectively, and Γ_S and Γ_B are the respective widths. Correlation lengths ξ , are defined as $\xi = 1/\Gamma$. For a perfect crystal, the presence of an average surface would give rise to a delta-function sharp component¹⁴. For the present case, with a finite bulk correlation length, we model the sharp component with a Lorentzian-squared function¹⁰ and constrain the width of this component to be equal to the width of the bulk orbital order superlattice reflection, $\Gamma_S = 0.0055 \text{ \AA}^{-1}$.

Taking a close look at the $T=170 \text{ K}$ data, we see that at large Q_z , the broad component has a much greater integrated intensity than the sharp component, while at small Q_z , the sharp component dominates. This is the expected behavior for a nearly smooth surface. Note that while the broad component is much broader than the sharp component, it is not as broad as would be

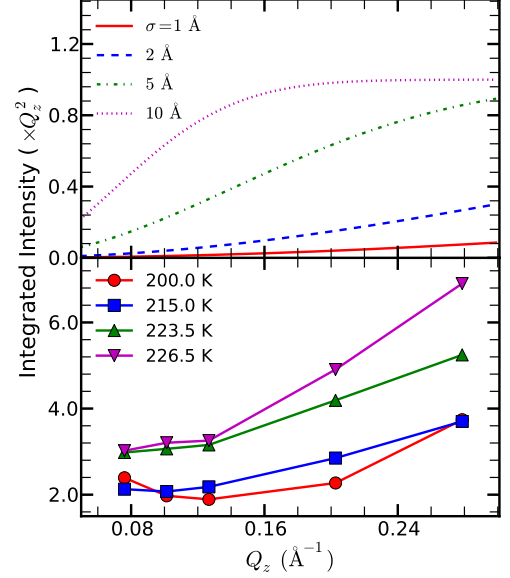


FIG. 3: (color online) (Top panel) Calculation of the Q_z dependence of the integrated intensity of the broad component for various values of the surface roughness, σ . (Bottom panel) Integrated intensity of the broad component as measured at several values of Q_z along the orbital truncation rod and for several temperatures. In each case, the integrated intensity is scaled by Q_z^2 to emphasize the high Q_z behavior. At temperatures approaching the bulk ordering temperature the measured integrated intensity increases faster with Q_z , indicative of an increased surface roughness.

expected if this was a line cut through the tails of the orbital Bragg peak (bottom panel, Fig. 1), that is both the sharp and broad components are associated with the orbital truncation rod, and hence reflect the properties of the orbital surface. At low temperatures, we find that the in-plane correlation length of the orbital surface is $1/\Gamma_B = 13 \text{ \AA}$, significantly shorter than the bulk correlation length ($1/\Gamma_S = 180 \text{ \AA}$), and in agreement with earlier work¹⁰.

We now discuss the temperature dependence of that surface upon warming through the bulk orbital order transition. The $T = 223.5 \text{ K}$ data of Fig. 2 already reveal dramatic changes from the low temperature lineshape. Specifically, there is no longer any evidence of a sharp component at any Q_z , and the broad component is both broader and more intense than it was at low temperatures.

As mentioned previously, for a rough surface, Q_x cuts perpendicular to the orbital truncation rod show a distinctive shape, composed of a broad and sharp component with integrated intensities for the broad and sharp component (I_S and I_B respectively) given by¹⁴:

$$I_S \propto \frac{1}{q_z^2} \exp(-\sigma^2 q_z^2), \quad (2)$$

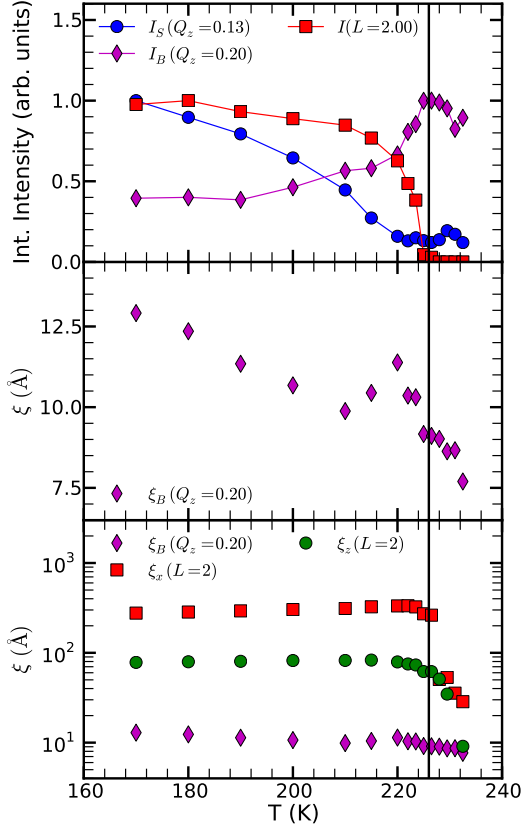


FIG. 4: (color online) (Top panel) Temperature dependence of the integrated intensity of the bulk orbital order superlattice reflection (red squares) measured at $L = 2$, the integrated intensity of the sharp component of the orbital truncation rod measured at $Q_z = 0.13 \text{ \AA}^{-1}$ (blue circles) and the broad component measured at $Q_z = 0.2 \text{ \AA}^{-1}$ (magenta diamonds). (Middle panel) Temperature dependence of the correlation length as measured on the broad component of the orbital truncation rod at $Q_z = 0.2 \text{ \AA}^{-1}$. (Bottom panel) Temperature dependence of the correlation lengths of the bulk orbital order superlattice reflection measured along the Q_z and Q_x directions (green circles and red squares respectively) and the correlation length as measured on the broad component of the orbital truncation rod at $Q_z = 0.2 \text{ \AA}^{-1}$.

$$I_B \propto \frac{1}{q_z^2} [1 - \exp(-\sigma^2 q_z^2)], \quad (3)$$

where σ is the surface roughness, and q_z is related to Q_z by the relation $\vec{Q} = \vec{G} + \vec{q}$ where \vec{G} is a reciprocal lattice point. The top panel of Fig 3 shows the calculated Q_z dependence of the integrated intensity of the broad component for a number of values of the surface roughness, σ , in Ångströms. All integrated intensities are scaled by Q_z^2 to emphasize the large Q_z behavior. From these simulations, we can see that as the roughness, σ is increased

the integrated intensity of the sharp component falls and the integrated intensity of the broad component increases for a given value of Q_z .

The bottom panel of Fig 3 shows experimentally measured data of the integrated intensity of the broad component as a function of Q_z for various temperatures. In comparison with the top panel of Fig. 3, we can see that at low temperature the scaled intensity is weak at high Q_z , indicative of a small surface roughness while the roughness increases rapidly as the temperature approaches the bulk melting temperature.

Figure 4 shows the evolution of the whole surface behavior in detail. In the top panel, the temperature dependence of the integrated intensity of the bulk superlattice Bragg peak ($L = 2$), the sharp component of the surface scattering, measured at $Q_z = 0.13 \text{ \AA}^{-1}$, and the broad component as measured at $Q_z = 0.2 \text{ \AA}^{-1}$, are shown. As the bulk orbital ordering transition is approached, the amplitude of the bulk superlattice peak decreases, disappearing at $T_{OO} = 226 \text{ K}$. The integrated intensity of the sharp component falls faster than the bulk orbital order Bragg peak and becomes indistinguishable from zero at $T = 222 \text{ K}$, i.e. below T_{OO} . In contrast, the integrated intensity of the broad component smoothly *increases*. The correlation length of the bulk orbital order is also shown, measured along the Q_z and Q_x directions, in the bottom panel of Fig. 4, along with the correlation length as measured on the broad component, along the Q_x direction. The latter is also plotted on a linear scale in the middle panel of Fig. 4. These data show that at low temperatures, the bulk orbital order is anisotropic, with the larger correlation length in the Q_x direction. This correlation length is larger than that of the broad component, indicative of a larger in-plane correlation length in the bulk compared to the orbital surface, again emphasizing that the surface orbital order is different from the bulk. As the temperature is raised, the correlation length of the bulk orbital reflection remains constant until T_{OO} at which point it rapidly decreases, becoming isotropic above the transition. In stark contrast, the correlation length of the broad component decreases steadily as the temperature is raised (middle panel, Fig. 4), indicative of a slow reduction of the in-plane interfacial correlation length. Above T_{OO} , the correlation lengths of the bulk orbital order Bragg reflection and the broad component become almost equal.

In summary, our data show the sharp component decreasing and reaching zero below the bulk melting temperature while at the same time the broad component of the interfacial scattering increases in a characteristic, Q_z -dependent way.

III. DISCUSSION

Before discussing the significance of these experimental results, it is useful to first discuss what the possible behavior for the orbital surface might be, on approaching

the bulk orbital order phase transition. One possibility is that of *surface freezing*, in which an ordered region exists at the surface of a disordered bulk. Soft matter systems such as liquid crystals¹⁷ and alkanes^{2,3} exhibit such behavior. A second, more common, scenario is that of surface melting (or pre-melting). Surface melting manifests itself as a disordered, liquid-like, region on the surface of a material, which grows in thickness upon approaching the bulk transition temperature from below¹⁸. In principle, electronic surfaces could exhibit either of these behaviors. In the study of magnetic surfaces, for example, there have been various experimental observations of differing surface and bulk magnetic phase transitions^{19,20}. On the theoretical side, it was found that for the ferromagnetic Ising model, - a model that has been used for orbital order in the manganites²¹ - it is possible to obtain either surface melting *or* surface freezing behavior, depending on the ratio of the exchange interactions for the surface and the bulk²². The question is then, which of these scenarios is the relevant one for the orbital surface discussed here?

The data presented above reveal very different behavior for the electronic surface and the bulk orbital order on warming through the bulk orbital ordering transition: At $T = 170$ K, well below the bulk transition temperature, the orbital surface is well defined but rougher than the crystal chemical surface, and has a shorter correlation length than the bulk orbital order. This situation is shown pictorially in Fig. 5(a) where we represent the different correlation lengths by regions of blue and yellow shading.

As the temperature is increased, the integrated intensity of the sharp component falls and the integrated intensity of the broad component increases, indicating that the interfacial width, or roughness, is increasing. Further, the correlation length measured on the broad component is found to steadily decrease, in contrast to the correlation length of the bulk orbital order, which remains constant throughout this temperature regime. This implies that the in-plane correlation length at the orbital surface is decreasing, while the bulk correlation length is unchanged.

At a temperature just below the bulk orbital order phase transition, the integrated intensity of the sharp component has dropped below detectable levels, and the broad component completely dominates, indicating that there is no average orbital surface at this temperature and that the orbital surface has melted. This is shown pictorially in Fig. 5(b). It is important to note that at this temperature, the bulk is still as well correlated as it was at low temperatures: Thus, this is a case of electronic surface melting.

Increasing the temperature further, one crosses the bulk phase transition and the bulk correlation lengths decrease to have approximately the same magnitude as the interfacial correlation length. In the absence of a surface, this implies that the orbital order exists as fluctuations in a disordered background. This case is shown in

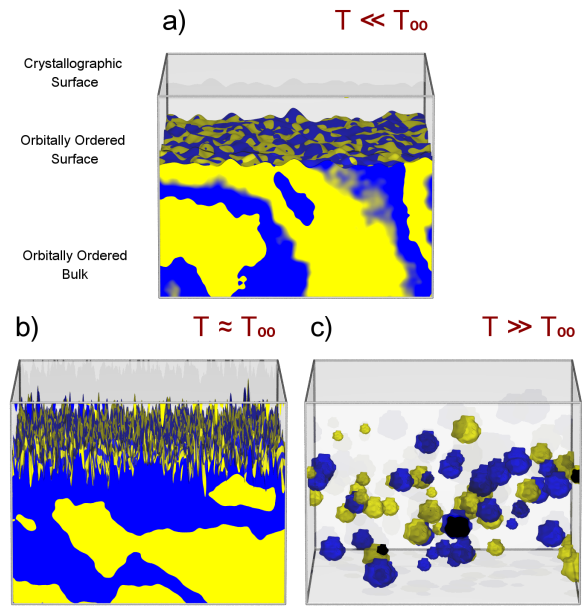


FIG. 5: (color online) Schematic representation of the crystallographic surface, the orbital surface and the orbitally ordered bulk for (a) $T \ll T_{oo}$, (b) $T \approx T_{oo}$ and (c) $T \gg T_{oo}$. The size of the blue and yellow regions in the orbitally ordered bulk represent schematically the correlation length of the orbital order in the bulk. The roughness of the orbital surface is shown as the height variations of the shaded (blue and yellow) surface and the in-place correlation length by the size of the shaded surface regions. The relative size of the colored regions are physically correct, both within each temperature snapshot and from temperature to temperature, as determined from the x-ray scattering data analysis.

Fig. 5(c). Further increasing the temperature causes the size of these fluctuations to decrease along with the integrated intensity. We note that Larochelle *et al.*²³ found that such short range fluctuations exist up to room temperature. This extremely short correlation length is also observed in $\text{La}_{1-x}\text{Sr}_{1+x}\text{MnO}_4$ with $x < 0.5$ ²³ which may suggest that this value may be representative of an intrinsic length-scale for the smallest fluctuation supported in the high temperature phase.

IV. CONCLUSIONS

We conclude by noting that this observation of electronic surface melting has potentially profound implications on the physics of strongly correlated materials and their applications in any device. Our results show that, at least for this system, the electronic surface becomes increasingly rough and less well defined on warming, and vanishes below the bulk ordering temperature. Materials with electronic surfaces that behave in this way could be problematic in devices operating at finite temperature. For example, colossal magnetoresistance²⁴ is a potentially very useful property. However, in man-

ganites, this effect requires the system to operate close to the bulk transition temperature. The present work shows that this temperature corresponds to the roughest orbital surface, which could be a problem for electron transport across that surface. Further, the properties of any nano-scaled device are likely to be dominated by the surface / interface behavior. Continuing with the CMR example, the stark difference between the surface and bulk means that at the nanoscale, CMR may manifest in a very different form - if at all. Finally, we comment that while the data presented here applies only to the orbital surface of LSMO, the implications of this work are likely to extend much further. For example, we note that much electronic information about strongly correlated systems is obtained from inherently surface sensitive techniques such as STM and ARPES. For systems that exhibit electronic surface melting, such techniques would measure the melted, rough layer, not the true bulk behavior. Our results suggest that future experimental and theoretical investigations of the temperature dependence of electronic surfaces are to be encouraged.

The work at Brookhaven was supported by the U.S. Department of Energy, Division of Materials Science, under Contract No. DE-AC02-98CH10886. Use of the Advanced Photon Source was supported by the U.S. Department of Energy, Basic Energy Sciences, Office of Science, under Contract No. W-31-109-Eng-38. Work in Japan was supported by the Ministry of Education, Culture, Sports, Science and Technology of Japan (KAKENHI 21740274,19052002)

-
- ¹ J. Dash, A. Rempel, and J. Wettlaufer, *Rev. Mod. Phys.* **78**, 695 (2006).
 - ² B. Ocko, X. Wu, E. Sirota, S. Sinha, O. Gang, and M. Deutsch, *Phys. Rev. E* **55**, 3164 (1997).
 - ³ X. Wu, E. Sirota, S. Sinha, B. Ocko, and M. Deutsch, *Phys Rev Lett* **70**, 958 (1993).
 - ⁴ P. Crouchman and W. Jesser, *Nature* **269**, 481 (1977).
 - ⁵ Z. Wang, J. Petroski, T. Green, and M. El sayed, *J. Phys. Chem. B* **102**, 6145 (1998).
 - ⁶ V. Levitas and K. Samani, *Nature Communications* **2**, 284 (2011).
 - ⁷ S. Okamoto and A. Millis, *Nature* **428**, 630 (2004).
 - ⁸ J. Freeland, K. Gray, L. Ozyuzer, P. Berghuis, E. Badica, J. Kavich, H. Zheng, and J. Mitchell, *Nature Mat.* **4**, 62 (2005).
 - ⁹ J. Chakhalian, J. Freeland, G. Srajer, J. Stremper, G. Khaliullin, J. Cezar, T. Charlton, R. Dalgliesh, C. Bernhard, G. Cristiani, et al., *Nature Phys.* **2**, 244 (2006).
 - ¹⁰ Y. Wakabayashi, M. Upton, S. Grenier, J. P. Hill, C. Nelson, J.-W. Kim, P. Ryan, A. Goldman, H. Zheng, and J. Mitchell, *Nature Mat.* **6**, 972 (2007).
 - ¹¹ A. Ohtomo and H. Hwang, *Nature* **427**, 423 (2004).
 - ¹² B. Sternlieb, J. Hill, U. Wildgruber, G. Luke, B. Nachumi, Y. Moritomo, and Y. Tokura, *Phys Rev Lett* **76**, 2169 (1996).
 - ¹³ Y. Murakami, H. Kawada, H. Kawata, M. Tanaka, T. Arima, Y. Moritomo, and Y. Tokura, *Phys Rev Lett* **80**, 1932 (1998).
 - ¹⁴ S. R. Andrews and R. A. Cowley, *J. Phys. C* **18**, 6427 (1985).
 - ¹⁵ I. K. Robinson and D. J. Tweet, *Reports on Progress in Physics* **55**, 599 (1992).
 - ¹⁶ H. You, *J Appl. Cryst.* **32**, 614 (1999).
 - ¹⁷ B. Swanson, H. Stragier, D. Tweet, and L. Sorensen, *Phys Rev Lett* **62**, 909 (1989).
 - ¹⁸ J. Frenken and J. Veen, *Phys Rev Lett* **54**, 134 (1985).
 - ¹⁹ K. Binder and P. Hohenberg, *Phys. Rev. B* **9**, 2194 (1974).
 - ²⁰ D. Mills, *Phys. Rev. B* **3**, 3887 (1971).
 - ²¹ A. Moreo, M. Mayr, A. Feiguin, S. Yunoki, and E. Dagotto, *Phys Rev Lett* **84**, 5568 (2000).
 - ²² C. Tsallis and A. Chame, *J Phys-Paris* **49**, 1619 (1988).
 - ²³ S. Larochelle, A. Mehta, L. Lu, P. Mang, O. Vajk, N. Kaneko, J. Lynn, L. Zhou, and M. Greven, *Phys. Rev. B* **71**, 024435 (2005).
 - ²⁴ S. Jin, T. Tiefel, M. McCormack, R. Fastnacht, R. Ramesh, and L. Chen, *Science* **264**, 413 (1994).